Detection of trap charge in small molecular organic bulk heterojunction solar cells

Debdutta Ray,* Lorenzo Burtone, Karl Leo, and Moritz Riede
Institut für Angewandte Photophysik, Technische Universität Dresden, 01062 Dresden, Germany
(Received 9 July 2010; published 7 September 2010)

We detect and measure the trap charges in a small molecular bulk heterojunction solar cell under operating conditions. The trap-charge density is estimated from capacitance measurements with light incident on the sample. At high intensities ($\sim$1 sun, 100 mW/cm^2), the trapped charge concentration leads to a spatial distortion of the electric field in the device. The lower limit of the trap-charge density is estimated to be 6×10^{16} cm^{-3}. The frequency dependence of the capacitance suggests that the charges are trapped in a manifold of deep states present in the energy gap of the semiconductors. The distortion of the electric field by this trap charge affects the charge-carrier collection efficiency.

DOI: 10.1103/PhysRevB.82.125204 PACS number(s): 72.80.Le, 88.40.jr, 73.50.Gr, 84.37.+q

I. INTRODUCTION

The power conversion efficiency of organic bulk heterojunction (BHJ) solar cells depends on the percentage of light absorbed in the active layer, photocarrier generation efficiency, carrier collection efficiency, and energy at which the charges are extracted.[1–5] Of these, the carrier collection efficiency is determined by the carrier mobility, carrier trapping times, and electric field in the sample.[6–12] The photocarrier generation, unlike in many inorganic semiconductors, is not spontaneous in these systems due to the tight binding of the electrons and holes in the form of excitons. Usually a heterojunction is required to achieve efficient exciton dissociation.[3] Nevertheless, the free carrier generation rate has been found to be dependent on the electric field.[13–15] The electric field, thus, plays an important role in determining the major solar-cell parameters in an organic solar cell. The electric field has been observed to be spatially constant for relatively low intensity illumination in single-layer organic devices.[7,9] The linear dependence of the carrier collection efficiency on electric field leads to such a conclusion. The total photocurrent (PC) may, however, vary superlinearly with the applied bias since the carrier generation efficiency may have an electric field dependence.[7,8]

The effect of the electric field on the carrier collection and the carrier generation efficiency can be found from electric field induced photoluminescence quenching and photocurrent-voltage measurements. In BHJ solar cells, the photocarrier generation takes place dominantly in the bulk of the sample. For low intensity illumination, the space-charge density is not large enough so as to influence the electric field.[7,9] Hence the total electric field, F, in the device can be written as $(V-V_{bi})/L$. Here V is the applied bias voltage, V_{bi} is the built-in voltage, and L is the thickness of the device. The charge-carrier collection length (assuming a drift model) can be written as $\mu\tau F$, where μ is the carrier mobility and τ is the carrier trapping time.[7,11,16] Apart from simulations which involve solving analytically the Poisson and the continuity equations simultaneously, analytical models also support the experimental observations of the charge-carrier collection efficiency as a function of electric field.[11,16,17] This picture is, however, modified once the carrier concentrations are increased, for example, in a solar cell under typical operating conditions. Although the basic framework of the models remains the same, one has to now take into account the effect of the trapped and space charges on the electric field in the sample. This has a direct bearing on the carrier collection efficiency and, hence, the power conversion efficiency of the solar cell.

The formation of trapped and space charge has been formulated in the analytical model of Goodman and Rose which has been successfully used in describing the photocurrent behavior in organic materials.[6,8,17] Later models have tried to spatially map the electric field in the device.[7,9] The presence of a space charge has been experimentally verified, albeit indirectly, by analyzing the photocurrent behavior as a function of applied voltage bias in organic solar cells.[6] The model of Goodman and Rose was used to understand the photocurrent behavior.[6,17] Although this model does not take into account the Poisson equation, the model predicts the photocurrent-voltage relation in the case of trapped or space charges.

In this work, we observe directly the presence of trap charge in ZnPc:C60 bulk heterojunction organic solar cells using capacitance measurements. The lower limit of the trap-charge density is estimated from capacitance-voltage measurements. From the frequency dependence of the capacitance, we observe that these states lie deep in the energy gap between the electron- and hole-transport levels.

II. EXPERIMENT

Single-layer bulk heterojunction devices are fabricated by codepositing zinc phthalocyanine (ZnPc, TCI Europe) and C60 (BuckyUSA) under high vacuum conditions (base pressure $<10^{-8}$ mbar) on indium tin oxide (ITO) coated glass substrates. In the devices either a thin layer of Au (10 nm, semitransparent) or p-dopant NDP9 (Novaled AG, Dresden, Germany) (2 nm) was deposited on ITO to change the built-in potential of the device. The introduction of a dopant or metal with a different Fermi level compared to ITO does not change the electronic properties of the active material and was done so as to demonstrate that capacitance measurement of trap-charge density is possible in devices with different architectures and built-in voltages. The proprietary p-dopant NDP9, which was used for better processability,

can also be replaced by the well-known molecule tetrafluoro-tetracyano-quinodimethane (F4-TCNQ) or by WO3 for similar results.[18,19] The ZnPc and C60 were purified at least twice using train sublimation. A typical device geometry is ITO/Au (10 nm)/ZnPc:C60 (1:2 volume ratio) (100 nm)/Al(100 nm). The donor/acceptor (D/A) ratio was so chosen since this lead to devices with high efficiencies.[20] The devices investigated here do not have doped hole-transport layers or doped electron-transport layers, used in the best cells, in order to keep the device as simple as possible.[20,21] In this way, the capacitance measures the response of the active layer. All devices have an active layer thickness of 100 nm and an area of 6.5 mm^2. The devices were encapsulated after deposition and were measured in a glove box with humidity and oxygen content less than 1 ppm. The capacitance was measured in dark as well as when the devices were illuminated using a solar simulator (Steuernagel) operating at Air Mass 1.5 Global (AM 1.5G). The maximum light intensity was 1 sun (100 mW/cm^2). Lower intensities were achieved by using neutral density filters. The device was illuminated through the ITO electrode. The capacitance was measured as a function of applied bias and frequency using a HP4284A LCR meter. In this paper, forward bias is defined as positive voltage applied to the ITO electrode. The current-voltage characteristics were measured using a Keithley-236 sourcemeter.

III. RESULTS AND DISCUSSION

Figure 1(a) shows the capacitance (C) as a function of frequency (f) for a ITO/Au (10 nm)/ZnPc:C60 (1:2 volume ratio) (100 nm)/Al(100 nm) device for different illumination intensities. The measurement was carried out at 0 V bias voltage. Figure 1(b) shows the phase of the current during the measurement. The phase is 90° for a pure capacitor and 0° for a pure resistor. Analysis of capacitance data was restricted to that with phase more than 10° to minimize errors associated with the measurement. The device is dominantly resistive when the phase is smaller than 10°. The capacitance in Fig. 1(a) increases with the decrease in modulation frequency for 1 sun and 23.6% sun incident intensities. For intensities smaller or equal to 6.9% of 1 sun, the change is negligibly low. The capacitance increases from 2.8 nF (geometrical capacitance) to 3.5 nF at 10 kHz frequency for 1 sun illumination intensity. The capacitance below 10 kHz cannot be measured with high accuracy since the phase falls off to 10° at 10 kHz. The dark capacitance is equal to the geometric capacitance proving that the sample is depleted in the dark. This is expected since the BHJ layer is intrinsic and undoped. The applied electric field in such a case is spatially uniform over the length of the sample. For zero applied bias, the electric field is equal to the built-in field.[22] In this case, the built-in voltage results from the Fermi-level difference of the contact electrodes.[22–24] The capacitance is dependent on the intensity of light incident on the device and increases with the increase in illumination intensity. The capacitance is a measure of the electric field alignment in a device. For example, the capacitance of a p-n junction is a measure of the depletion width since the modulation of charge takes place at the depletion edge.[1] The increase in capacitance is

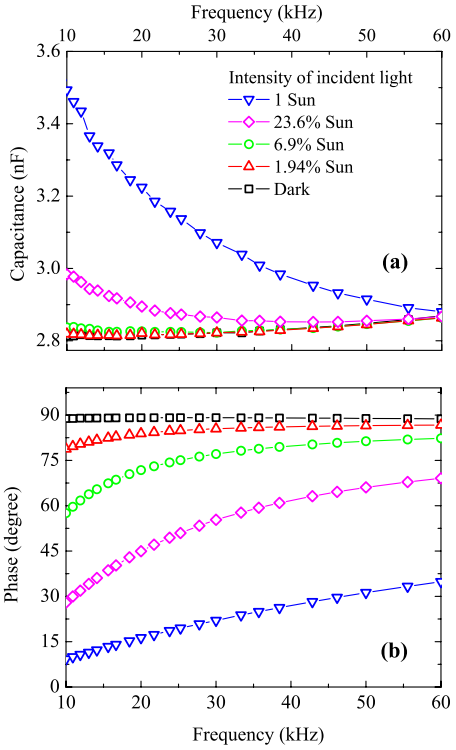

FIG. 1. (Color online) The capacitance (at 0 V bias voltage) as a function of modulation frequency is shown in (a) while the phase of the measured current as a function of frequency is shown in (b). The device geometry is ITO/Au(10 nm)/ZnPc:C60(1:2)/Al. The measurement is made at different incident light intensities. The connecting lines are used as a guide for the eyes.

evidence of the formation of space charge or trapped charge in the sample which leads to the distortion of the uniform electric field in the sample. Figure 2(a) shows the capacitance as a function of voltage (V) measured in the same device at 10 kHz frequency. 10 kHz was chosen as the optimum frequency since at lower frequencies, the capacitance cannot be measured with high accuracy for 1 sun intensities. Moreover, at higher frequencies lesser number of states respond which leads to smaller change in capacitance. The frequency dependence of the capacitance is discussed in detail later. Figure 2(b) shows the corresponding phase of the measurement. The capacitance depends on the intensity of light and decreases with the increase in reverse bias voltage. At 0 V bias and for 1 sun intensity, the phase is around 12° and is well within measurement limits. The current-voltage characteristics of the device are shown in Fig. 3 for various illumination intensities. The open circuit voltage of the device is around 0.12 V for this device. The reverse current increases with voltage implying that the not all carriers are collected.

The behavior of the capacitance as a function of frequency and voltage can be understood as follows. The photocurrent of the device depends on a number of factors. This includes the carrier collection efficiency. The carrier collection efficiency dictates the electric field at which total carrier collection will occur. The larger the carrier collection efficiency, the better the fill factor of a solar cell.[12] The carrier collection length "schubweg" is given by the product of the

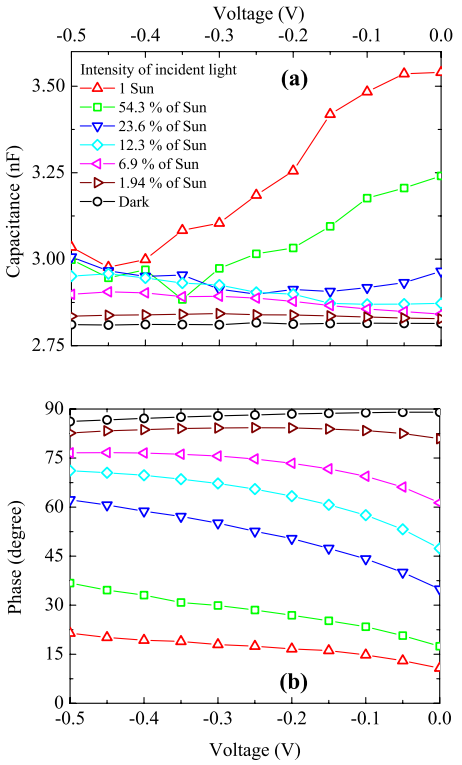

FIG. 2. (Color online) The capacitance (at 10 kHz modulation frequency) as a function of applied bias is shown in (a) while the corresponding phase of the measured current is shown in (b). The device geometry is ITO/Au(10 nm)/ZnPc:C60(1:2)/Al. The measurement is made at different light intensities. The connecting lines are used as a guide for the eyes.

carrier mobility (μ), carrier trapping time (τ), and the electric field (F). There have been many postulations regarding the electric field and its spatial structure in such devices. Goodman and Rose have analytically solved for the photocurrent in insulators by assuming carrier trapping in deep states.[17] These carriers lead to distortion of the electric field. The field distortion is proportional to the ratio of the majority and minority carrier $\mu\tau$ product.[17] The majority carrier in an insulator is defined by the carrier with the larger $\mu\tau$ product.

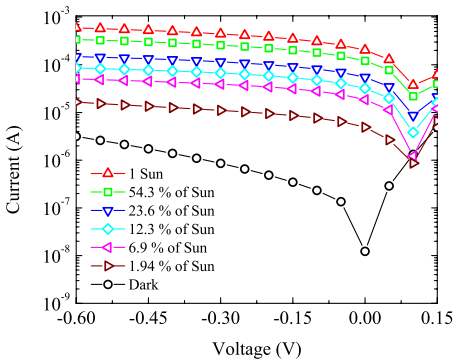

FIG. 3. (Color online) A plot of the current as a function of voltage for a ITO/Au(10 nm)/ZnPc:C60(1:2)/Al device under dark and illuminated conditions. The measurement is made at different light intensities. The connecting lines are used as a guide for the eyes.

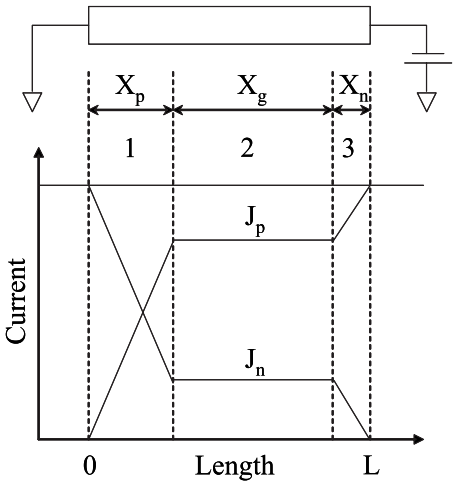

FIG. 4. The figure shows the spatial variation in the hole and the electron photocurrent (J_p and J_n, respectively) in a device working under reverse bias conditions (maximum gain of 1). The device can be broken up roughly into three regions. Regions 1 and 3 are current generating regions whose lengths (X_p and X_n. respectively) are determined by the $\mu\tau F$ product of holes and electrons (Refs. 7 and 17). F is the electric field. Region 2 is a stationary region and does not contribute to the total photocurrent. With increasing reverse bias, region 2 (with length X_g) decreases and vanishes at voltages where all photogenerated carriers are collected. The photocurrent saturates when all carriers are collected.

The electrons get collected at the positively biased contact while the holes are collected at the negatively biased contact. According to their theory, the electric field near the interface where the minority carriers are collected gets modified in steady state. This analysis can be used to understand the photocurrent in many devices including bulk heterojunction organic cells. Mihailetchi *et al.* have used this theory to detect space-charge-limited photocurrent where they deduce the formation of the space charge from the functional form of the photocurrent [$PC \propto (V - V_{bi})^{1/2}$].[6] In later works, the photocurrent has been simulated numerically by simultaneously solving the Poisson and the continuity equations. It has been found that the electric field distortion is negligible for small incident intensities ($\ll$1 sun).[7,9] The total photocurrent is, however, still given by the total carrier collection length assuming uniform field under small intensities. This means that the space-charge or trap-charge formation is not large enough to affect the electric field significantly. This is not reflected in the model of Goodman and Rose since it does not take into account the Poisson equation.[17] It is, hence, expected that the effect of the space charge or trap charges on the electric field and therefore on the capacitive response will depend on the incident illumination intensity. Larger intensities should have a more enhanced effect on the capacitance.

The capacitance in Fig. 2(a) is at maximum at 0 V and decreases approaching the geometric capacitance with the increase in reverse bias. The capacitance depends on the intensity of light being incident on the sample. This result can be understood as follows. The device can be broken up into three sections when illuminated.[7,17] This is shown in Fig. 4.

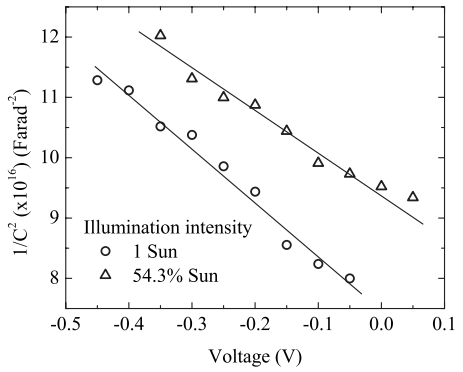

FIG. 5. A plot of $1/C^2$ vs voltage for two illumination intensities: 1 sun and 54.3% sun. The trap carrier concentration is estimated to be around 6×10^{16} cm^{-3} by fitting these plots to the profiler formula (Ref. 28).

Regions 1 and 3 are photocurrent generating regions. Region 2 in the center is a stationary region and does not contribute to the photocurrent. This is because the carrier generation rate is equal to the carrier recombination rate in region 2. Therefore, the individual hole and electron photocurrent in region 2 is constant. The lengths of the regions 1 (X_p) and 3 (X_n) are given by the carrier collection length of the majority and the minority carriers, respectively. In this case, the hole is shown to have a larger carrier collection length. With increasing electric field, the length of region 2 (X_g) decreases and tends to zero when all the carriers are collected. For the case where the stationary region 2 is nonzero, the photocurrent will increase with increasing applied bias. The photocurrent is proportional to the total carrier collection length of the holes and the electrons. In reverse bias, i.e., when the contacts are noninjecting and hence the maximum photocurrent gain is 1, the photocurrent saturates with voltage when all carriers are collected. For small incident intensities, there is no observable electric field distortion. At large intensities, space charge or trap charge can lead to changes in the electric field and this is what that is detected by capacitance. The decrease in capacitance with reverse voltage is due to the increasing carrier collection at higher fields. The electric field distortion is due to carriers filling up trap states present in the active layer.[25–27] At higher fields, the trapping probability decreases with the increase in carrier collection efficiency. The trap-charge concentration can be modeled by the profiler formula,[28]

$$N_{CV} = -\frac{C^3}{\varepsilon q A^2}\left[\frac{dC}{dV}\right]^{-1}. \quad (1)$$

The N_{CV} in such a case is the concentration of the occupied trapping centers or the trap-charge concentration. In Eq. (1), A is the area of the device, q the electronic charge, and ε the dielectric constant. Figure 5 shows the $1/C^2$ vs V plot for 1 sun and 0.5 sun intensities. N_{CV} is found to be around 6×10^{16} cm^{-3} from the slope. The carrier collection length is where the electric field is maximum assuming an unequal electron and hole $\mu\tau$ product.[17] The capacitance measures this region and hence the capacitance will have a functional form similar to that of the profiler formula with homogenous charge distribution. At −0.5 V, most of the carriers are collected and the capacitance approaches the geometric capacitance. The slight deviation from the geometric capacitance for higher illumination intensities is probably due to trapped charges in deep states which cannot escape under these electric field and temperature conditions. The role of gap states to the observed capacitance is analyzed below.

The increase in illuminated capacitance with the decrease in frequency, as shown in Fig. 1(a) is evidence that the trapping sites are spread out in energy with respect to the transport levels.[28–30] When the traps form a manifold of states distributed in the energy gap of the semiconductor, only those that has a response time faster than the modulation signal will be able to change their charged states.[28] These are the states which will contribute to the capacitance. The response time is proportional to $\exp(\Delta E/kT)$, where ΔE is the energy difference between the trap state and the transport level.[28] With the decrease in frequency, deeper states will start to respond thereby increasing the measured capacitance. The capacitance should be independent of frequency at sufficiently low frequencies where all states respond.[28] However, the device becomes increasingly resistive at lower frequency and hence it is not possible to measure the capacitance at low frequencies under illumination. The N_{CV} that is determined from the C-V plot is, therefore, a lower limit to the concentration of the trap-charge density. It must be noted that the N_{CV} measured at 1 and 0.5 sun are similar which indicates that the charge density is due to trapping sites and the capacitance measures the concentration of these states. At low intensities, the number of photogenerated carriers is low and hence the distortion in the electric field is small as very few of these trapping sites are filled. At large reverse bias, the field is relatively uniform across the semiconductor since all carriers are collected. We note that the intensity dependence of the photocurrent is linear (not shown). According to the model of Goodman and Rose, this observation suggests that trap charges are responsible for the distortion of the electric field.[17]

Figure 6(a) shows the capacitance as a function of voltage for a ITO/p-dopant NDP9(2 nm)/ZnPc:C60 (1:2) (100 nm)/Al device. Figure 6(b) shows the phase as a function of voltage for the different illuminating intensities. A thin layer of p-dopant NDP9 was used to increase the open circuit voltage of the device. The p-dopant leads to an effective Fermi level which is deeper in energy compared to Au. This enhances the built-in voltage.[22,23] With the increase in the open circuit voltage, the partial carrier collection regime in voltage shifts from the third quadrant of the current-voltage plot (as observed in the previous case with Au contact) to the fourth quadrant. This is shown in Fig. 7 which shows the photocurrent as a function of voltage for different illumination intensities. This effect also gets reflected in the capacitance voltage plot where we observe that the capacitance maximum is at 0.35 V. This is consistent with the explanation of the capacitance given above. In this case, the increase in the open circuit voltage, which is a direct consequence of the larger built-in voltage, means that the electric field is larger for a given bias (below the open circuit voltage) compared to the device without a p dopant on the ITO. Thus, the carrier collection efficiency is higher for the same voltage. The capaci-

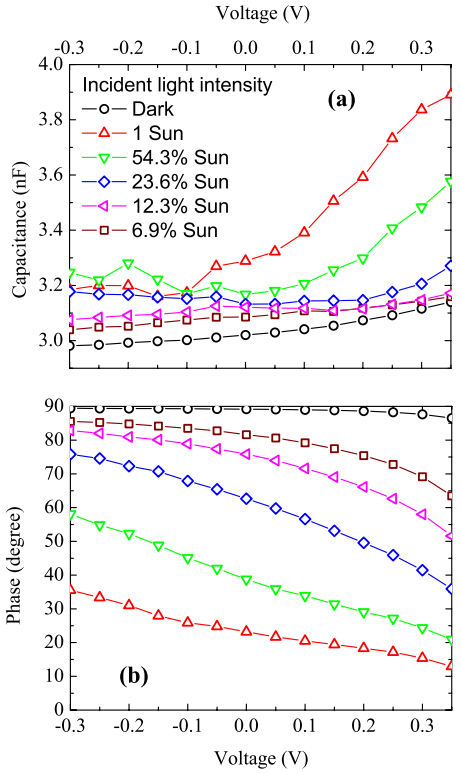

FIG. 6. (Color online) The capacitance as a function of applied bias is shown in (a) while the corresponding phase of the measured current is shown in (b). The device geometry is ITO/*p*-dopant NDP9(2 nm)/ZnPc:C60(1:2)/Al. The measurement is made at different light intensities. The connecting lines are used as a guide for the eyes.

tance decreases and approaches the geometric capacitance at around −0.15 V. The photocurrent also approaches saturation at this voltage. This is expected since at total carrier collection, the electric field is relatively uniform across the length of the device. Thus, we observe that for devices with the same materials constituting the active region, the effect of the trap charge shifts from the third to the fourth quadrant with the shift in the open circuit voltage. It must be noted

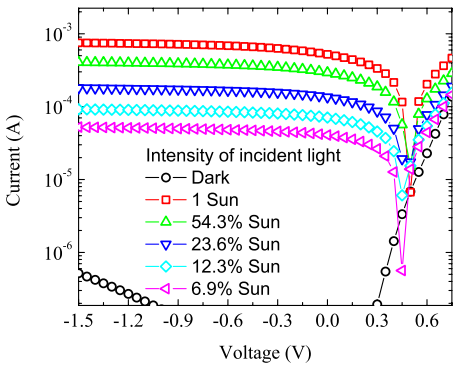

FIG. 7. (Color online) A plot of the current as a function of voltage for a ITO/*p*-dopant NDP9(2 nm)/ZnPc:C60(1:2)/Al device under dark and illuminated conditions. The measurement is made at different light intensities. The connecting lines are used as a guide for the eyes.

that the dark capacitance is slightly larger (3.1 nF) than the geometric capacitance (3.0 nF) at 0.35 V bias. There could be two possible reasons for this behavior. One reason is that at 0.35 V forward bias, there is carrier injection from the contacts in dark (Fig. 7) which can influence the capacitance. The other possible reason is that there may be dopant diffusion from the ITO/*p*-dopant (2 nm) contact which can *p*-dope ZnPc near this contact. In this case, it is possible to observe a capacitance slightly larger than the geometric capacitance because of a lightly doped Schottky-type junction. However, this effect is observed to be rather weak and has very little influence on the illuminated capacitance.

The effect of this nonuniform electric field plays a very important role in solar-cell efficiencies since the device operates in the fourth quadrant of the current-voltage regime. The carrier collection efficiency is directly proportional to the electric field.[1,9,11] Formation of trap charge can lead to a decrease in the carrier collection efficiency. It is, hence, necessary to have devices where the trap-charge density is minimized. From frequency-dependent measurements, we conclude that the charge density is formed by carriers trapped at trapping centers. These trapping centers are spread out in energy in the energy gap which is observed from the increase in capacitive response with decreasing frequency.[28] The depth of the traps can be calculated only if the attempt-to-escape frequency is known.[28] Assuming an attempt-to-escape frequency generally observed in inorganic semiconductors (10^{11} Hz), we estimate that the trap levels extend deeper than 0.4 eV (calculated at response frequency of 10 kHz) from the transport level. The donors and the acceptors which forms the percolating paths for carrier collection is randomly spread out in a bulk heterojunction.[2,31,32] The ensuing small overlap in wave functions of nearest-neighbor molecules can lead to such states where the charges may be trapped. The D/A interface may also act as a trapping site. These states being deep in energy will determine the carrier trapping times of the material. The dominant carrier recombination mechanism in organic bulk heterojunction solar cells is being debated where bimolecular recombination could be one of the possibilities.[9,33,34] The presence of deep traps suggests that trap-induced recombination may also play a major role.[34–37] The presence of deep traps has also been observed in doped organic materials.[25,34] It has been suggested that these states may be intrinsic to the material or may form via impurities or polarization corrections with the introduction of another material or dopant.[25] At large carrier (photocarrier or electrode injected) concentrations, these charged states will affect the electric field. The dark current has been reported to be affected by the presence of traps.[38,39] From illuminated capacitance measurements, we have been able to estimate the lower limit of their concentration. In order to measure the total trap state concentration, it is necessary to make low-frequency capacitance measurements. This is not possible in our cases since the samples become dominantly resistive at low frequencies when illuminated with intensities on the order of 1 sun. The capacitance will be independent of the modulated frequency at low frequencies when all trap states respond. There can be a number of factors which may give rise to such states. If they are due to impurity then this problem may be overcome by purification. On the other hand, if

they are formed at the D/A interface or if they are intrinsic to the material then it is necessary to look for new materials with lower trap states. The morphology or crystalline structure can also give rise to traps. Now that the active layer is desired to have crystalline order in order to facilitate charge extraction, it becomes important to study the trap state formation as a function of the morphology of the film.

IV. CONCLUSIONS

We have used capacitance measurements to directly observe the presence of trapped charges in an operating organic bulk heterojunction solar-cell active layer. The charge density is formed by carriers trapped in states located deep in the energy gap of the molecules. The trap charge influences the electric field in the sample which in turn influences the carrier collection efficiency. The lower limit of the density of these trap states is estimated to be around 6×10^{16} cm^{-3}. The trap states may be formed at the D/A acceptor interface or in the constituent material. To enhance device efficiency, it is necessary to minimize the number of such states.

ACKNOWLEDGMENTS

The research leading to these results has received funding from the European Community's Seventh Framework Programme (FP7/2007-2013) under Grant Agreement No. 212311 of the ONE-P project.

*Corresponding author; debdutta.ray@iapp.de

[1] S. M. Sze, *Physics of Semiconductor Devices*, 2nd ed. (Wiley-Interscience, New York, 1981), pp. 245–249.
[2] F. Yang and S. R. Forrest, ACS Nano **2**, 1022 (2008).
[3] J. J. M. Halls, C. A. Walsh, N. C. Greenham, E. A. Marseglia, R. H. Friend, S. C. Moratti, and A. B. Holmes, Nature (London) **376**, 498 (1995).
[4] M. Niggemann, M. Riede, A. Gombert, and K. Leo, Phys. Status Solidi A **205**, 2862 (2008).
[5] M. Riede, T. Mueller, W. Tress, R. Schueppel, and K. Leo, Nanotechnology **19**, 424001 (2008).
[6] V. D. Mihailetchi, J. Wildeman, and P. W. M. Blom, Phys. Rev. Lett. **94**, 126602 (2005).
[7] D. Ray, M. P. Patankar, G. H. Dohler, and K. L. Narasimhan, J. Appl. Phys. **100**, 113727 (2006).
[8] D. Ray, M. P. Patankar, N. Periasamy, and K. L. Narasimhan, J. Appl. Phys. **98**, 123704 (2005).
[9] L. J. A. Koster, E. C. P. Smits, V. D. Mihailetchi, and P. W. M. Blom, Phys. Rev. B **72**, 085205 (2005).
[10] C. Waldauf, M. C. Scharber, P. Schilinsky, J. A. Hauch, and C. J. Brabec, J. Appl. Phys. **99**, 104503 (2006).
[11] R. S. Crandall, J. Appl. Phys. **53**, 3350 (1982).
[12] P. Schilinsky, C. Waldauf, J. Hauch, and C. J. Brabec, J. Appl. Phys. **95**, 2816 (2004).
[13] V. D. Mihailetchi, L. J. A. Koster, J. C. Hummelen, and P. W. M. Blom, Phys. Rev. Lett. **93**, 216601 (2004).
[14] C. L. Braun, J. Chem. Phys. **80**, 4157 (1984).
[15] V. Gulbinas, D. Hertel, A. Yartsev, and V. Sundström, Phys. Rev. B **76**, 235203 (2007).
[16] R. S. Crandall, J. Appl. Phys. **54**, 7176 (1983).
[17] A. M. Goodman and A. Rose, J. Appl. Phys. **42**, 2823 (1971).
[18] J. Meyer, S. Hamwi, S. Schmale, T. Winkler, H.-H. Johannes, T. Riedl, and W. Kowalsky, J. Mater. Chem. **19**, 702 (2009).
[19] S. Reineke, F. Lindner, G. Schwartz, N. Seidler, K. Walzer, B. Lüssem, and K. Leo, Nature (London) **459**, 234 (2009).
[20] J. Drechsel, B. Maennig, F. Kozlowski, M. Pfeiffer, K. Leo, and H. Hoppe, Appl. Phys. Lett. **86**, 244102 (2005).
[21] B. Maennig, J. Drechsel, D. Gebeyehu, P. Simon, F. Kozlowski, A. Werner, F. Li, S. Grundmann, S. Sonntag, M. Koch, K. Leo, M. Pfeiffer, H. Hoppe, D. Meissner, N. S. Sariciftci, I. Riedel, V. Dyakonov, and J. Parisi, Appl. Phys. A **79**, 1 (2004).
[22] I. H. Campbell, T. W. Hagler, D. L. Smith, and J. P. Ferraris, Phys. Rev. Lett. **76**, 1900 (1996).
[23] D. Ray, M. P. Patankar, N. Periasamy, and K. L. Narasimhan, Synth. Met. **155**, 349 (2005).
[24] G. G. Malliaras, J. R. Salem, P. J. Brock, and J. C. Scott, J. Appl. Phys. **84**, 1583 (1998).
[25] D. Ray and K. L. Narasimhan, J. Appl. Phys. **103**, 093711 (2008).
[26] O. Tal, Y. Rosenwaks, Y. Preezant, N. Tessler, C. K. Chan, and A. Kahn, Phys. Rev. Lett. **95**, 256405 (2005).
[27] I. N. Hulea, H. B. Brom, A. J. Houtepen, D. Vanmaekelbergh, J. J. Kelly, and E. A. Meulenkamp, Phys. Rev. Lett. **93**, 166601 (2004).
[28] J. D. Cohen and D. V. Lang, Phys. Rev. B **25**, 5321 (1982).
[29] G. I. Roberts and C. R. Crowell, J. Appl. Phys. **41**, 1767 (1970).
[30] C. R. Crowell and K. Nakano, Solid-State Electron. **15**, 605 (1972).
[31] K. Maturová, S. S. van Bavel, M. M. Wienk, R. A. J. Janssen, and M. Kemerink, Nano Lett. **9**, 3032 (2009).
[32] B. P. Rand, J. Xue, S. Uchida, and S. R. Forrest, J. Appl. Phys. **98**, 124902 (2005).
[33] P. Langevin, Ann. Chim. Phys. **28**, 289 (1903).
[34] M. M. Mandoc, F. B. Kooistra, J. C. Hummelen, B. de Boer, and P. W. M. Blom, Appl. Phys. Lett. **91**, 263505 (2007).
[35] W. Shockley and W. T. Read, Jr., Phys. Rev. **87**, 835 (1952).
[36] R. N. Hall, Phys. Rev. **87**, 387 (1952).
[37] R. S. Crandall, in *Semiconductors and Semimetals*, edited by J. I. Pankove (Academic Press, Orlando, 1984), Vol. 21, Part B, pp. 245–297.
[38] M. Stößel, J. Staudigel, F. Steuber, J. Blässing, J. Simmerer, and A. Winnacker, Appl. Phys. Lett. **76**, 115 (2000).
[39] P. E. Burrows, Z. Shen, V. Bulovic, D. M. McCarty, S. R. Forrest, J. A. Cronin, and M. E. Thompson, J. Appl. Phys. **79**, 7991 (1996).